ANTIFERROMAGNETIC RESONANCE IN $RbMnF_3$ UNDER AXIAL STRESS*

D. E. Eastman, R. J. Joenk, and D. T. Teaney
IBM Watson Research Center, Yorktown Heights, New York
(Received 8 July 1966)

Magnetoelastic constants of antiferromagnetic $RbMnF_3$ were determined at 4.2°K from the stress and field dependence of AFMR frequency: $b_1 = 1.5\times 10^6$ and $b_2 = 0.17\times 10^6$ erg/cm^3; linewidths are accounted for by inhomogeneous strain broadening. Spin-lattice strain coefficients for Mn^{++} in a regular F^- octahedron were derived as $G_{11} = 0.32$ and $G_{44} = -0.073$ (cm^{-1}/ion) after correcting the b's for magnetic dipolar contributions.

We have studied magnetoelastic coupling in antiferromagnetic $RbMnF_3$ by observing shifts in antiferromagnetic resonance (AFMR) frequency and changes in AFMR line shape with the application of axial stress. The magnetoelastic constants have been determined at 4.2°K. The elastic constants have also been determined so that the results can be interpreted in terms of the actual lattice distortion. By computing the contribution of dipole interactions to the magnetoelastic constants, the strain-induced crystal field splitting has been determined; the spin-lattice coefficients[1] thus obtained are the first to be reported for Mn^{2+} surrounded by a regular octahedron of F^- and, furthermore, since the lattice is uniform, the local strain is known unambiguously. Finally, we conclude that the observed linewidth results from inhomogeneous strain broadening.

The effect of stress on the applied field for AFMR at 23 Gc/sec is shown in Fig. 1. In this instance, the pressure is along the [001] cube edge and the applied field is along [100] (upper curve) and [110] (lower curve) perpendicular to the stress. The physical origin of the large shift is readily visualized. The magnetoelastic energy adds to the normal anisotropy energy, and its contribution may be treated as a stress-dependent effective anisotropy field H_σ; the corresponding field for AFMR is $[2H_E(H_A+H_\sigma)]^{1/2}$. In $RbMnF_3$,[2] the exchange field H_E is about 10^6 Oe, the intrinsic anisotropy field H_A is about 4 Oe, and the induced anisotropy field H_σ is comparable to H_A. Large effects are thus to be expected. In comparison with a ferromagnet having the same magnetoelastic constants, the flopped-state AFMR is shifted by an amount H_E/H_0 greater than the ferromagnetic resonance would be.

Quantitatively we have calculated the static-equilibrium spin orientation and AFMR frequencies for a two-sublattice antiferromagnet characterized by cubic crystalline anisotropy and magnetoelastic energy of the form

$$E = K_1[(\alpha_1^2\alpha_2^2 + \text{c.p.}) + (\beta_1^2\beta_2^2 + \text{c.p.})] + b_1[(\alpha_1^2 + \beta_1^2)\eta_{11} + \text{c.p.}] + b_2[\alpha_1\alpha_2 + \beta_1\beta_2)\eta_{12} + \text{c.p.}], \quad (1)$$

where α_1 and β_1 are the direction cosines of the sublattice magnetizations,

$$\eta_{ij} = (1-\tfrac{1}{2}\delta_{ij})(\partial u_i/\partial x_j + \partial u_j/\partial x_i)$$

is the strain tensor, b_1 and b_2 are the magnetoelastic constants, and c.p. denotes cyclic permutations. K_1 is the usual magnetocrystalline anisotropy constant which is negative for $RbMnF_3$ and corresponds to an anisotropy field $H_A = -4K_1/(3M_S)$ when the sublattices lie along the equilibrium [111] directions; M_S is the sublattice magnetization. Full details of the solutions for general applied fields and stress for both field-dependent and field-independent modes will be published elsewhere.[3] We present here only a discussion appropriate to the results shown in Fig. 1.

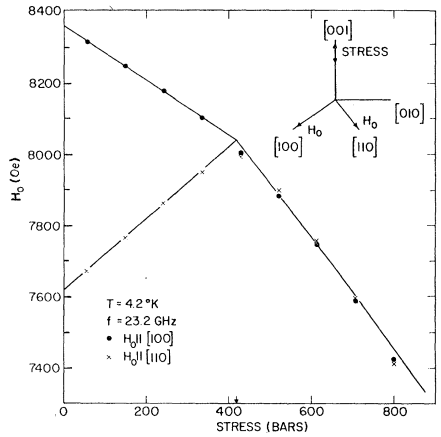

FIG. 1. AFMR resonance frequency versus [001] stress; $H_E = 0.89\times 10^6$ Oe, $H_A = 3.8$ Oe, $H_N = 2.22$ Oe, and $b_1 = 1.5\times 10^6$ erg/cm^3.

We find experimentally that compression in the z direction ($\eta_{33} < 0$) produces a stress anisotropy with an easy axis in the z direction; that is, $b_1 > 0$. For the case of an applied field $H_0 > (2H_E H_A)^{1/2}$ along [100], two equivalent domains are formed having sublattice magnetizations parallel and antiparallel to [011] and [0$\bar{1}$1]. Under [001] compression the static-equilibrium magnetization vectors rotate away from the face diagonals into the z direction. The AFMR frequency is given by

$$(\omega_\perp/\gamma)^2 = H_0^2 + 2H_E H_N - (\tfrac{3}{2})H_E H_A + H_E H_{\sigma 1} \quad (2)$$

for the stress range $0 \leq H_{\sigma 1} \leq (\tfrac{3}{2})H_A$. Here

$$H_{\sigma 1} = -2b_1\sigma_{33}/(c_{11}-c_{12})M_s \quad (3)$$

is the effective field induced by a z-axis stress σ_{33}. The c's are the usual elastic constants. H_N is the Mn^{55} hyperfine field (9.4/T Oe).

There is a discontinuity in the slope of the resonance field versus stress curve when $H_{\sigma 1}$ equals $(\tfrac{3}{2})H_A$. In the stress range $H_{\sigma 1} \geq (\tfrac{3}{2})H_A$, the magnetoelastic anisotropy predominates over the intrinsic cubic anisotropy to produce a single-domain uniaxial antiferromagnet having a resonance frequency

$$(\omega_\perp/\gamma)^2 = H_0^2 + 2H_E H_N - 3H_E H_A + 2H_E H_{\sigma 1}. \quad (4)$$

Similarly, when the applied field is along [110], the two domains rotate away from [$\bar{1}$11] and [1$\bar{1}$1] into the z direction. The frequency in the stress range $0 \leq H_{\sigma 1} \leq (\tfrac{3}{2})H_A$ is

$$(\omega_\perp/\gamma)^2 = H_0^2 + 2H_E H_N + 2H_E H_A - (\tfrac{4}{3})H_E H_{\sigma 1}. \quad (5)$$

Again, a discontinuity occurs when $H_{\sigma 1} = (\tfrac{3}{2})H_A$. For $H_{\sigma 1} \geq (\tfrac{3}{2})H_A$, the resonance frequency is given by Eq. (4) for all H_0 perpendicular to the z axis. The solid curves in Fig. 1 are based on Eqs. (2), (4), and (5), the adjustable parameters being b_1 and H_A.

The second magnetoelastic constant b_2 is found from resonance shifts under [110] stress. The results are similar to the [001] case described and are characterized by an effective field $H_{\sigma 2} = -(b_2\sigma_{12})/(c_{44}M_s)$ which appears in combinations with $H_{\sigma 1}$ in resonance equations like those above.

The magnetoelastic constants measured at 4.2°K for $RbMnF_3$ are given in Table I. To obtain these values we have used the theoretical value $M_s = 304$ Oe, the measured value $H_E = 0.89 \times 10^6$ Oe, and the measured room-temperature

Table I. Magnetoelastic constants of $RbMnF_3$ at 4.2°K in units of 10^6 erg/cm^3.

	Measured	Dipolar	Δb
b_1	1.5	−1.65	3.15
b_2	0.17	1.10	−0.93

elastic constants (in units of 10^{11} dyne/cm^2) $c_{11} = 10.45$, $c_{12} = 3.32$, and $c_{44} = 3.00$. Also given in Table I are the calculated magnetic dipolar contributions to b_1 and b_2. The differences Δb between the observed constants and the dipolar term give the contribution of the crystal field splitting to the magnetoelastic energy. Using the noncubic spin Hamiltonian defined by Feher[1] and the lattice parameter $a_0 = 4.24$ Å, we obtain the spin-lattice strain coefficients

$$G_{11} = (4/15)a_0^3\Delta b_1 = 0.32 \text{ cm}^{-1},$$

$$G_{44} = (\tfrac{1}{5})a_0^3\Delta b_2 = -0.073 \text{ cm}^{-1}.$$

While single-ion epr data for Mn^{2+} in, say, $RbZnF_3$ do not exist, it is interesting to note that our results are similar in magnitude and sign to Feher's measurements on Mn^{2+} in MgO, which are $G_{11} = 1.5$ cm^{-1} and $G_{44} = -0.32$ cm^{-1}. Further numerical comparison seems unwarranted in view of the lack of a quantitative theoretical account of even the basic single-ion effects observed by Feher.

From the study of magnetoelastic coupling we are able to conclude that the AFMR linewidth observed in $RbMnF_3$ at 4.2°K is the result of static broadening by inhomogeneous strains in the crystal. Typical line shapes are shown in Fig. 2 for various amounts of stress corresponding to the lower branch of the field versus stress curve in Fig. 1, i.e., σ along [001]

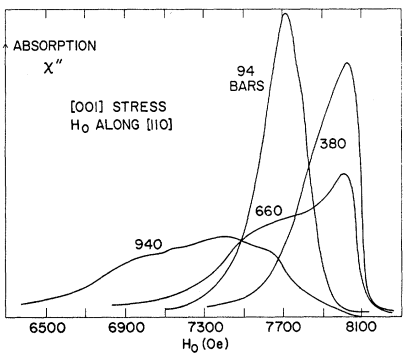

FIG. 2. Microwave absorption versus field under applied stress.

and H_0 along [110]. For zero stress the line is very nearly Gaussian in shape, corresponding to an envelope of uniform mode resonances arising from a random distribution of domains in various states of local strain. The local strain could presumably pin the domain as well as shift the AFMR frequency. The AFMR can be broadened by this mechanism in an antiferromagnet because the lack of a net moment eliminates the dipole narrowing[4] which is present in a ferromagnet; in other words, no net long-range dipole fields are available to couple different regions together so that they assume a common resonance frequency.

In general, the observed linewidth is proportional to the slope, $dH_0/d\sigma$, of the resonance field versus stress curve as would be expected if the random local strain were added to the over-all strain. Thus, the AFMR line is broader in the high-stress uniaxial regime than it is for $H_{\sigma 1} < (\frac{3}{2})H_A$. An extensive discussion will be published elsewhere.[3] We conclude the present account by pointing out the particularly striking example of strain broadening shown by the AFMR line at $H_{\sigma 1} \simeq (\frac{3}{2})H_A$ ($\sigma_{33} = -380$ bar) and $H_0 \| [110]$ in Fig. 2. At this point H_0 vs σ is a maximum, and the effect of inhomogeneous strain is to shift all domains to resonance fields less than $H_0 = [(\omega/\gamma)^2 - 2H_E H_N]^{1/2}$. The line is observed to cut off abruptly on the high-field side. From the steepness of this cutoff, we are able to estimate the linewidth of the uniform mode to be $\lesssim 5$ Oe. We have observed nonlinear AFMR absorption[5] in $RbMnF_3$ much like that reported by Heeger for $KMnF_3$,[6] and we conclude from this comparison that spin-wave linewidths are of the same order of magnitude as the uniform-mode linewidth.

We are grateful to A. M. Toxen for his assistance in the ultrasonic elastic-constant measurements.

*Work supported in part by U. S. Air Force Office of Scientific Research of the Office of Applied Research under Contract No. AF 49 (639)-1379.

[1]E. R. Feher, Phys. Rev. 136, A145 (1964).
[2]D. T. Teaney, M. J. Freiser, and R. W. H. Stevenson, Phys. Rev. Letters 9, 212 (1962).
[3]D. E. Eastman, Phys. Rev. 148, 530 (1966).
[4]A. M. Clogston, J. Appl. Phys. 29, 334 (1958).
[5]D. T. Teaney, J. S. Blackburn, and R. W. H. Stevenson, Bull. Am. Phys. Soc. 7, 201 (1962).
[6]A. J. Heeger, Phys. Rev. 131, 608 (1963).

FINE STRUCTURE IN THE DIRECT ABSORPTION EDGE OF DIAMOND*

R. A. Roberts, D. M. Roessler, and W. C. Walker
Department of Physics, University of California, Santa Barbara, California
(Received 20 June 1966)

Ultraviolet optical studies of diamond have been carried out over the past few years by several investigators.[1-4] There are several features of agreement in the various studies but also some important differences near 7, 9, 16, and 20 eV. In particular, a low-temperature investigation of the direct absorption edge near 7 eV by Clark, Dean, and Harris[3] (CDH) showed a strong sharpening of the 7-eV peak with a small energy shift when compared with the room-temperature measurement. This feature was interpreted by Phillips[5] as evidence for the existence of a hybrid exciton in diamond. The studies of Refs. 1, 3, and 4 also present evidence for interband structure between 8 and 9 eV. Because of the importance of diamond as a basic test of our understanding of covalent binding, it was decided to conduct additional studies of diamond at both room and liquid-nitrogen temperatures. In this note, reflectance data obtained from 5.5 to 11.5 eV will be reported.

Reflectance measurements on polished type-I and both cleaved and polished type-IIa diamonds were made. Measurements at near normal incidence (9°) were taken using a glass light pipe coated with sodium salicylate, which could be rotated to monitor the incident and reflected beams. The stainless-steel reflectometer was separated from the monochromator by a LiF window and maintained at a pressure of better than 10^{-7} Torr by means of a Vacion-titanium sublimation pumping system. A 1200-line/mm grating in a one-meter monochromator with 300-μ slits gave a resolution of 4 Å (0.015 eV) or better over the region measured. The light source used was a dc hydrogen-glow discharge in a boron-nitride capillary. Measurements